

Azimuthal angular distributions for two-colour three-photon ionization of hydrogen

M. Fifrig¹ and V. Florescu^{2,a}

¹ Department of Chemistry, University of Bucharest, Bd. Carol 13, Bucharest, 70346 Romania

² Department of Physics, University of Bucharest, Bucharest-Magurele, 76900 Romania

Received: 12 November 1997 / Accepted: 23 February 1998

Abstract. We study in some detail the photoelectron angular distributions in two-colour three-photon ionization of the ground state hydrogen atom in its dependence on the polarizations of the two electromagnetic fields. We treat the particular case of photons propagating in the same direction and having elliptic polarizations with the same axes. The azimuthal distributions presented refer to the electrons emitted with momenta orthogonal to the photons direction. The calculations are done in nonrelativistic dipole approximation, in velocity gauge, using third-order perturbation theory. We show that the photoelectron azimuthal angular distributions have a fourfold symmetry only for identical linear or circular polarizations. In all the other cases the distribution has a twofold symmetry.

PACS. 32.80.Rm Multiphoton ionization and excitation to highly excited states (e.g., Rydberg states)
– 32.80.Fb. Photoionization of atoms and ions

1 Introduction

The angular distributions of the ejected electrons in photoionization contain more information on the atomic system than the total cross-sections. The polarization of the electromagnetic field in one-colour photoionization has interesting effects in intense fields. This property was discussed first in the experimental work of Bashkansky *et al.* [1], reporting asymmetries in the distribution of ATI photoelectrons generated by elliptically polarized light for noble gas atoms like helium, krypton and xenon, in contrast to the fourfold symmetry characteristic to the case of linearly or circularly polarized light. Calculations do support the reduction of the symmetry in the azimuthal angular distribution: Basile *et al.* [2] has treated the twelve- and sixteen-photon ionization of hydrogen, and Trombetta *et al.* [3] the case of helium, ionized by the absorption of a number of photons between thirteen and seventeen. The reduction of the symmetry of the photoelectron angular distributions in multiphoton ionization due to elliptically polarized light was also explained and illustrated for the case of two-photon ionization by Lambropoulos and Tang [4] and by Muller [5].

All the results we have quoted refer to one colour processes. In the interaction with two electromagnetic fields, the polarization effects have been studied in a few cases. One of the considered processes is two-colour ionization, studied only for linear and circular polarizations [6, 7].

In this paper we consider the process of ionization of atomic hydrogen by absorption of three photons, one of frequency ω_1 and complex polarization \mathbf{s}_1 , the other two of frequency ω_2 and complex polarization \mathbf{s}_2 . Each polarization vector is normalized such that $\mathbf{s} \cdot \mathbf{s}^* = 1$. This process may be represented as

$$\text{H}(1s) + \gamma(\mathbf{s}_1, \omega_1) + 2\gamma(\mathbf{s}_2, \omega_2) \rightarrow \text{H}^+ + e^-(E_f, \mathbf{k}_f) \quad (1)$$

where $E_f = E_1 + \hbar\omega_1 + 2\hbar\omega_2$ (E_1 is the ground state energy). E_f and \mathbf{k}_f are, respectively, the energy and the asymptotic momentum of the final electron.

In a previous paper [8], we have reported analytic results for the three-photon 1s - continuum transition amplitude, valid in nonrelativistic dipole approximation, in velocity gauge, based on third-order perturbation theory. We have exploited these analytic expressions in a quantitative study [9] of the ionization described in equation (1), presenting results for the frequency dependence of the total cross-section and for several angular distributions, but only for linearly and (or) circularly polarized photons. The aim of this paper is an extension of our calculations in [9] to an investigation of the effects of photons polarizations on the electron angular distributions. We focus on a particular geometry, described in Section 2, where we present the structure of the corresponding photoelectron angular distributions. The results are shown and commented in Section 3.

^a e-mail: flor@barutu.fizica.unibuc.ro

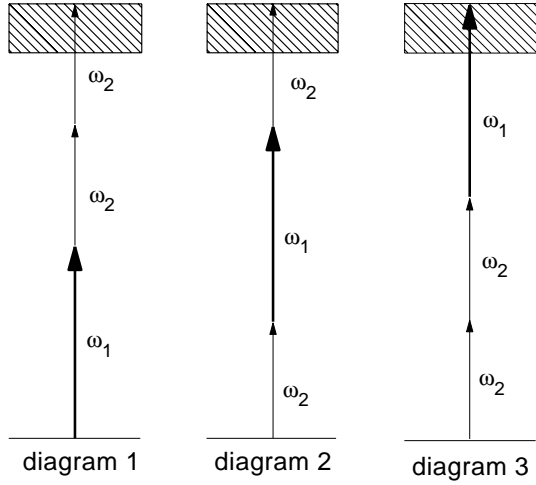


Fig. 1. Feynman diagrams associated to the process of ionization of the hydrogen atom initially in the ground state, by the absorption of three photons, two of the same frequency.

2 General equations for the angular distributions

For a ground state hydrogen atom in interaction with two monochromatic electromagnetic fields, in LOPT (lowest order perturbation theory), three Feynman diagrams of third order in the fine structure constant α are associated to the process in which three photons, two of them identical, are simultaneously absorbed (see Fig. 1). We consider here the particular regime $\omega_1 > \omega_2$, $\hbar\omega_1 + \hbar\omega_2 < |E_1|$, *i.e.*, the case in which the absorption of two photons with different frequencies is not sufficient for ionization. The conditions imposed do not exclude the possibility of ionization by absorption of two photons of frequency ω_1 , if $2\hbar\omega_1 > |E_1|$. The three-photon process is favoured by choosing the intensity of the field of frequency ω_2 higher than the intensity of the other field.

Azimuthal angular distributions of the electrons produced in two-colour three-photon ionization are evaluated here in dipole approximation and in the velocity gauge, using analytic equations we have derived previously [8]. We study here a particular case, in which: i) both photon beams propagate in the same direction, taken as the z axis; ii) the principal axes of the polarization state of the two beams are the same; iii) the ejected electron momentum is orthogonal on the photons direction. As a consequence of i) and ii) the polarization vectors of the photons are

$$\mathbf{s}_k = \mathbf{e}_x \cos \frac{\zeta_k}{2} + i\mathbf{e}_y \sin \frac{\zeta_k}{2}, \quad k = 1, 2, \quad (2)$$

where \mathbf{e}_x and \mathbf{e}_y denote the unit vectors along the common semimajor and semiminor axes of the ellipses described by the two electric fields. ζ_1 and ζ_2 are the *retardation angles* lying in the range $-\pi/2 \leq \zeta_k \leq \pi/2$. Each retardation angle ζ determines the helicity ($h = \sin \zeta$) and the ellipticity parameter ($\eta = \tan(\zeta/2)$) of the corresponding radiation field. The values $\zeta = 0$ and $\zeta = \pm\pi/2$ correspond, respectively, to linear and circular polarizations. When $h > 0$

the electric field vectors move clockwise in the $x-y$ plane (left elliptically polarized light). For $h < 0$ the electric field vectors move anticlockwise in the $x-y$ plane (right elliptically polarized light).

We denote by ϕ the azimuthal angle of the electron, measured counterclockwise from the positive x axis. In the conditions mentioned before, we find convenient to write the differential cross section divided by I_2^2 , with I_2 the intensity of the field of frequency ω_2 , as

$$I_2^{-2} \frac{d\sigma}{d\Omega} = \mathcal{K} [t_1 + t_2 \sin 2\phi], \quad (3)$$

making explicit the presence of the function $\sin 2\phi$. The quantities t_1 and t_2 depend also on ϕ , but contain only the function $\cos 2\phi$ or its powers, as follows:

$$\begin{aligned} t_1 = & (1 + \cos \zeta_1 \cos 2\phi) \left[4 \left| \left(b + \frac{c}{2} \right) \cos \zeta_2 + \frac{c}{2} \cos 2\phi \right|^2 \right. \\ & \left. + |c|^2 \sin^2 \zeta_2 \sin^2 2\phi \right] \\ & + 4(1 + \cos \zeta_2 \cos 2\phi) \cos \frac{\zeta_1 + \zeta_2}{2} \left[|a|^2 \cos \frac{\zeta_1 + \zeta_2}{2} \right. \\ & \left. + \operatorname{Re}(ac^*) \left(\cos \frac{\zeta_1 + \zeta_2}{2} + \cos \frac{\zeta_2 - \zeta_1}{2} \cos 2\phi \right) \right] \\ & + 8 \cos \zeta_2 \cos \frac{\zeta_1 + \zeta_2}{2} \\ & \times \left(\cos \frac{\zeta_2 - \zeta_1}{2} + \cos \frac{\zeta_1 + \zeta_2}{2} \cos 2\phi \right) \operatorname{Re}(ab^*), \end{aligned} \quad (4)$$

$$\begin{aligned} t_2 = & 2 \left(1 + \cos \zeta_1 \cos 2\phi \right) \sin(2\zeta_2) \operatorname{Im}(bc^*) \\ & + 2 \left(1 + \cos \zeta_2 \cos 2\phi \right) \sin(\zeta_1 + \zeta_2) \operatorname{Im}(ac^*) \\ & + 8 \cos \zeta_2 \cos \frac{\zeta_1 + \zeta_2}{2} \sin \frac{\zeta_2 - \zeta_1}{2} \operatorname{Im}(a^*b). \end{aligned} \quad (5)$$

The coefficients a , b , and c are given by equation (9) in our previous paper [9] and the coefficient \mathcal{K} has the expression

$$\mathcal{K} = \frac{\pi^2 \alpha}{Z^{14}} \left(\frac{a_0}{I_0} \right)^2 \frac{1}{k_1 k_2^4}.$$

We have denoted by $k_j = \hbar\omega_j/|E_1|$, $j = 1, 2$, the energies of the two kind of photons measured in $Z^2 \times \text{Rydberg}$; Z is the atomic number, α the fine structure constant, I_0 the atomic unit for field intensity, and a_0 the Bohr radius.

The equations (3)-(5) display the symmetry properties of the azimuthal angular distributions. First of all, the photoelectron angular distribution is invariant at the change $\phi \rightarrow \phi \pm \pi$. It is also invariant at the simultaneous changes $\zeta_1 \rightarrow -\zeta_1$, $\zeta_2 \rightarrow -\zeta_2$, and $\phi \rightarrow -\phi$. Due to the first invariance property, the azimuthal angular distribution presents a *twofold* rotational symmetry. The coefficient t_2 in equation (3), responsible for the reduction of the symmetry with respect to the polarization

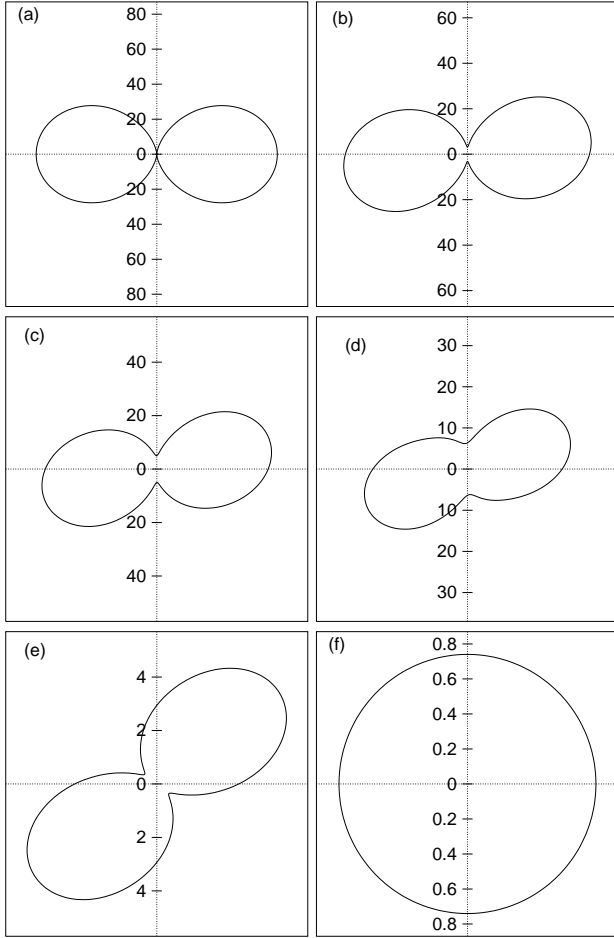


Fig. 2. Azimuthal angular distributions for ejected electrons (Eq. (6)), multiplied by the factor 10^{46} , for identical elliptic polarizations, for $\hbar\omega_1 = 5.5$ eV and $\hbar\omega_2 = 4.65$ eV (the third harmonic of Ti:Sapphire laser). Values of the retardation angle ζ are, going from (a) to (f), 0° , 25° , 35° , 50° , 75° , and 90° .

axis, vanishes for $\zeta_1 = \zeta_2 = 0$ (identical linear polarizations), $\zeta_1 = \zeta_2 = \pm\pi/2$ (identical circular polarizations), or $\zeta_1 = \pm\pi/2$ and $\zeta_2 = \mp\pi/2$ (orthogonal circular polarizations). In all these cases, the angular distribution is also invariant at the change $\phi \rightarrow -\phi$. Due to this supplementary invariance, the electron angular distribution has a fourfold rotational symmetry. The coefficient t_2 itself would vanish if the amplitudes a , b , and c were real, but this is not the case in the energy regime investigated here.

3 Numerical results

The nontrivial part of the numerical calculation is the evaluation of the amplitudes a , b and c in equations (4) and (5). We use for this purpose the analytic expressions derived in [8], which express these amplitudes as series of products of Gauss hypergeometric functions ${}_2F_1$ with a sum of several Appell functions F_1 (see also [9]).

We analyze here the dependence of the azimuthal angular distributions (Eqs. (3)-(5)) on the ellipticity and the

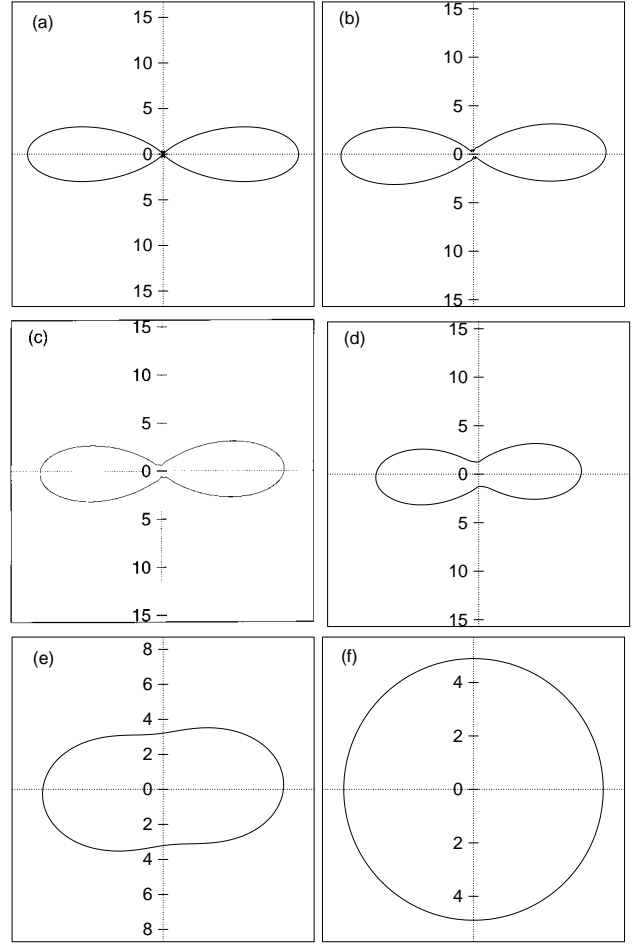


Fig. 3. Same as Figure 2a to f but for $\hbar\omega_1 = 8.05$ eV and $\hbar\omega_2 = 4.65$ eV.

frequencies of the two photon beams in some particular cases.

We consider first the case of *identical elliptic* polarizations, $\zeta_1 = \zeta_2 \equiv \zeta$, when equation (3) becomes

$$I_2^{-2} \frac{d\sigma}{d\Omega} = \mathcal{K} \left(1 + \cos \zeta \cos 2\phi \right) \times \left[4 \left| \left(a + b + \frac{c}{2} \right) \cos \zeta + \frac{c}{2} \cos 2\phi \right|^2 + |c|^2 \sin^2 2\phi \sin^2 \zeta + 2 \operatorname{Im} \left((a + b) c^* \right) \sin 2\zeta \sin 2\phi \right]. \quad (6)$$

For $\zeta = 0$ or $\pm\pi/2$ the angular distributions has a fourfold rotational symmetry and the equation (6) is in agreement with equation (11) in [9].

Results based on equation (6) are presented in Figures 2 and 3. The plotted quantity $I_2^{-2} d\sigma/d\Omega$, multiplied by the factor 10^{46} is shown for several values of the retardation angle ζ : 0° , 25° , 35° , 50° , 75° and 90° . In each case the values of the frequencies are chosen in the vicinity of a resonance. In the conditions of Figure 2, we are near the resonance located at 10.2 eV reached by the absorption of

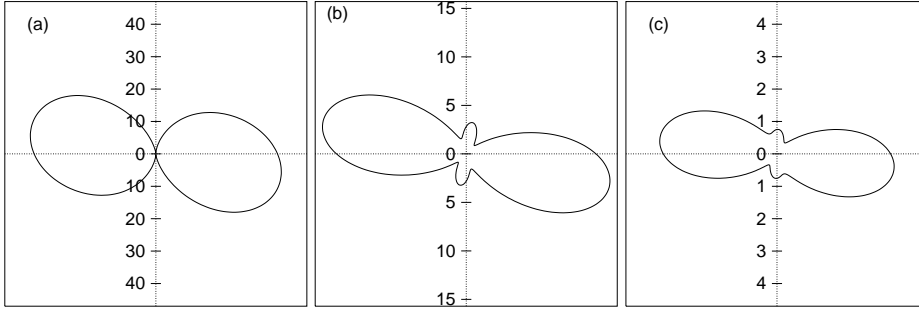


Fig. 4. Photoelectron azimuthal angular distributions (Eq. (7)), multiplied by the factor 10^{46} , for $\zeta_1 = -\pi/2$, $\zeta_2 = 0$, and $\hbar\omega_2 = 4.65$ eV. The values of the other photon energy are, going from (a) to (c), $\hbar\omega_1 = 5.5$ eV, 7.4 eV, 8.05 eV.

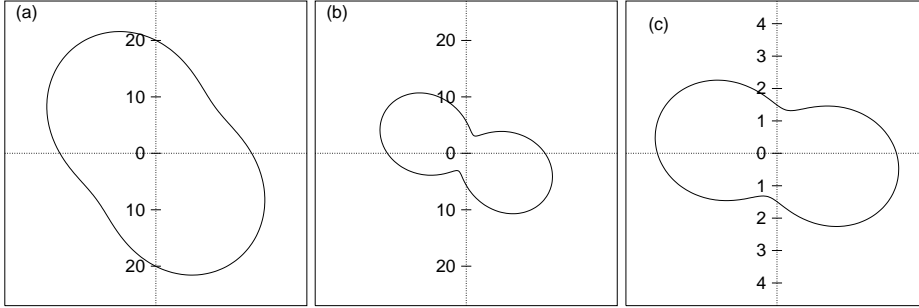


Fig. 5. Photoelectron azimuthal angular distributions (Eq. (8)), multiplied by the factor 10^{46} , for $\zeta_1 = 0$ and $\zeta_2 = -\pi/2$, and $\hbar\omega_2 = 4.65$ eV. The values of the other photon energy are the same as in Figures 4a,b and c.

two photons of energy 5.5 eV, and in those of Figure 3 near the resonance located at 12.75 eV, through the absorption of one photon of energy $\hbar\omega_1 = 8.05$ eV and one of energy $\hbar\omega_2 = 4.65$ eV (the third harmonic of Ti:Sapphire laser). The resonance 10.2 eV is due to the intermediate 2s state, while that of 12.75 eV to 4d intermediate state (see [9]). For $\zeta = 0^\circ$ (Fig. 2a) the fourfold symmetry holds, while for $\zeta \neq 0$ ($\zeta = 25^\circ$ in Fig. 2b) the polar diagram becomes asymmetric with respect to the polarization axes. A twofold symmetry holds for any ζ . The angles of maximum ejection are 0° and 180° for $\zeta = 0$. With the increasing of ζ , this angle rotates. The minima of the polar diagram at 90° and 270° for $\zeta = 0$ rotates very slowly with the increasing of ζ . The angular distribution broadens rapidly in the vicinity of $\zeta = 90^\circ$.

We notice that the asymmetric angular distribution reverses with the reversal of the sign of the light helicity.

The comparison between Figure 2 and 3 shows the role of the photon frequencies in the dependence of the photons ellipticity. The fourfold symmetry holds again when $\zeta = 0$ (Fig. 3a) and $\zeta = 90^\circ$ (Fig. 3f). In comparison with Figure 2, for the other values of the retardation angle ζ , the asymmetry is less pronounced and the angle of maximum ejection rotates very slowly. The azimuthal angular distribution broadens with the increase of ζ .

In Figures 4 and 5 the ellipticities of the two-photon beams are different. Figure 4 corresponds to the case $\zeta_1 = -\pi/2$ (right circular polarization) and $\zeta_2 = 0$ (linear polarization).

When $\zeta_1 = \pm\pi/2$ (+ for left and - for right circular polarization) and $\zeta_2 = 0$, equation (3) becomes

$$I_2^{-2} \frac{d\sigma}{d\Omega} = 4\mathcal{K} \left[|a+d|^2 \cos^2 \phi + |d|^2 \sin^2 \phi \mp \text{Im}(a^*d) \sin 2\phi \right], \quad (7)$$

with $d = b + c \cos^2 \phi$.

Figure 4 displays the azimuthal angular distribution of the ejected electrons given by equation (7) as polar diagrams, for $\hbar\omega_2 = 4.65$ eV (the third harmonic of Ti:Sapphire laser) and several values of the photon energy $\hbar\omega_1$: 5.5 eV in Figure 4a, 7.4 eV in Figure 4b and 8.05 eV in Figure 4c. Choosing these frequencies we are again near the resonance located at 10.2 eV (in Fig. 4a), near the one at 12.1 eV (in Fig. 4b) and that at 12.75 eV (in Fig. 4c). Here also, the plotted quantity is multiplied by the factor of 10^{46} . The curves in Figures 4b and 4c have secondary maxima due to the contribution of the intermediate d states in the corresponding resonances. With the increase of the frequency ω_1 the azimuthal distribution broadens. The polar diagrams from Figures 4a, b and c illustrate a strong dependence of the angular distribution on the photons frequencies, through the amplitudes a, b, c . We mention also that these asymmetric distributions reverse with a reversal of the sign of ζ_1 (change from left to right circular polarization).

If we interchange the photons polarizations in comparison with the case studied before, *i.e.*, we consider the case $\zeta_1 = 0$ and $\zeta_2 = \pm\pi/2$, equation (3) becomes

$$I_2^{-2} \frac{d\sigma}{d\Omega} = \frac{\mathcal{K}}{2} \left[4|a + c \cos^2 \phi|^2 + |c|^2 \sin^2 2\phi \mp 4 \text{Im}(a^*c) \sin 2\phi \right]. \quad (8)$$

In Figures 5a, b and c we take $\zeta_1 = 0$ and $\zeta_2 = -\pi/2$, and we keep the same values of the photons frequencies as in Figures 4a, b and c. The polar diagrams broaden in comparison with those from Figures 4a,b and c. This comparison illustrates the effect of the polarizations on the shape of the angular distributions.

In conclusion, in the case of two-colour three-photon ionization of hydrogen, for a particular geometry of the incident photons and of the photoelectron, and some values of the frequencies, we have illustrated how the ellipticity of the radiation not only modifies the symmetry of the electron angular distribution, but also its shape. In particular, the fourfold rotational symmetry occurring for identical linear or circular polarizations is reduced to a twofold symmetry. The photon polarization effects can be augmented or diminished by the values of the photon frequencies.

This work is part of the EC contract CIPD CT940025 and of the contract 949/1997 of the Romanian CNCSU. The numerical calculations were performed on the workstation HP-715 of the Computer Center of the Quantum and Statistical Physics Group (Bucharest-Magurele), a donation of the SOROS Foundation. The authors are grateful to A. Maquet for useful discussions, encouragements and criticism of this work.

References

1. M. Bashkansky, P.H. Bucksbaum, D.W. Schumacher, *Phys. Rev. Lett.* **60**, 2458 (1988).
2. S. Basile, F. Trombetta, G. Ferrante, *Phys. Rev. Lett.* **61**, 2435 (1988).
3. F. Trombetta, G. Ferrante, S. Basile, *J. Phys. B* **21**, L539 (1988).
4. P. Lambropoulos, X. Tang, *Phys. Rev. Lett.* **61**, 2506 (1988).
5. H.G. Muller, G. Petite, P. Agostini, *Phys. Rev. Lett.* **61**, 2507 (1988).
6. S. Bivona, R. Burlon, C. Leone, G. Ferrante, *Nuovo Cimento D* **11**, 1751 (1989).
7. A. Cionga, *Rom. J. Phys.* **38**, 483 (1993).
8. A. Cionga, M. Vatasescu, M. Fifrig, V. Florescu, *Rom. Rep. Phys.* **56**, 441 (1994).
9. M. Fifrig, A. Cionga, V. Florescu, *J. Phys. B* **30**, 2599 (1997).